Nonadiabatic effects in a generalized Jahn-Teller lattice model: Heavy and light polarons, pairing, and the metal-insulator transition

Eva Majerníková,[1,2,*] J. Riedel,[1] and S. Shpyrko[1,†]
[1]*Department of Theoretical Physics, Palacký University, Tř. 17. listopadu 50, CZ-77207 Olomouc, Czech Republic*
[2]*Institute of Physics, Slovak Academy of Sciences, Dúbravská cesta, SK-84 228 Bratislava, Slovak Republic*
(Received 5 June 2001; revised manuscript received 29 January 2002; published 23 April 2002)

The self-consistent ground state polaron potential of one-dimensional lattice of two-level molecules with spinless electrons and two dispersionless phonon modes with linear coupling and quantum phonon-assisted (nonadiabatic) transitions between the levels is found anharmonic in phonon displacements. As a function of these, the potential shows a crossover from two nonequivalent broad minima to a single narrow minimum which correspond to the positions of the levels in the ground state. Generalized variational approach respecting the mixing of levels (reflection) via a variational parameter implies prominent nonadiabatic effects: (i) In the limit of the symmetric $E\otimes e$ Jahn-Teller situation they cause transition between the regime of the predominantly one-level ''heavy'' polaron and a ''light'' polaron oscillating between the levels due to phonon assistance with almost vanishing polaron displacement. Vanishing polaron selflocalization implies *enhancement of the electron transfer* due to decrease of the ''heavy'' polaron mass (undressing) at the point of the transition. There can occur *pairing of "light" polarons* due to exchange of virtual phonons. *Continuous transition to new energy ground state close to the transition from "heavy" polaron phase to "light" (bi)polaron phase occurs*. In the ''heavy'' phase, we have found anomalous (anharmonic) enhancements of quantum fluctuations of the phonon coordinate, conjugated momentum and their product in the ground state as functions of the effective coupling which reach their maxima at $E\otimes e$ JT symmetry. They decrease rapidly to their harmonic values as soon as the ''light'' phase is stabilized. (ii) Nonadiabatic dependence of the polaron mass (Debye-Waller screening) on the optical phonon frequency appears. (iii) The contribution of Rabi oscillations to the transfer enhances significantly quantum shift of the insulator-metal transition line to higher values of the critical effective electron-phonon coupling supporting so the metallic phase. In the $E\otimes e$ JT case, insulator-metal transition can coincide with the transition between the ''heavy'' and the ''light'' (bi)polaron phase only at certain (strong) effective electron-phonon interaction.

DOI: 10.1103/PhysRevB.65.174305 PACS number(s): 71.38.−k, 73.90.+f, 42.50.Dv, 05.30.−d

I. INTRODUCTION

Recently an interest in electron-phonon models was renewed owing to high-T_c-superconducting layered cuprates and fullerene compounds that exhibit structure instability due to strong Jahn-Teller effect accompanied by an evident isotope effect.[1–6] Here, nonadiabatic (quantum) fluctuations were found to be important since the majority of the superconducting structures exhibited low values of the Fermi energy, comparable to the phonon energy and large isotope effect. Nonadiabatic fluctuations also appeared relevant in manganese-based perovskites at Jahn-Teller (JT) distortion assisted by formation of JT polaron and causing oxygen isotope effect and a collosal magnetoresistance.[3] The mechanism of nonadiabatic pairing was proposed by several authors: Manini *et al.*,[7] Zheng and co-workers,[8,9] Kresin and co-workers,[4,5] Pietronero and co-workers[10] for C_{60} compounds and recently also for the challenging new superconductor MgB_2.[11] Theories of pairing mechanism based on polarons (bipolarons), including also electron-electron interactions evoked great interest as well.[12–14]

Nonadiabatic fluctuations affect the charge transport because they reduce the polaron band narrowing[8,9,15] (i.e., polaron renormalization of the electron mass). Fluctuations increase near the phase transitions[16–19] destroying the phase coherence for weak interactions and shifting the critical couplings to higher values. However, numerical simulations of different lattice models (Fradkin and Hirsch,[16] Borghi *et al.*,[17] McKenzie *et al.*[18]) prove a general statement that the resulting quantum fluctuations are much more pronounced than those obtained by variational approaches, e.g., by Zheng *et al.*,[8] Feinberg *et al.*,[15] Lo and Sollie,[20] and Chen *et al.*[21] Namely, the quantum shift of critical values of the electron-phonon coupling from numerical simulations to higher values (preferring so the metallic phase) was shown to exceed considerably their variational values. Moreover, the numerical simulations of two-level lattice electron-phonon systems in one dimension by Feinberg *et al.*[15] and by Borghi *et al.*[17] evidence anomalous increase of quantum fluctuations of the phonon coordinate and of the conjugated momentum as well as anomalous increase of their product referring to enhancement of anharmonic effects. The simulations manifest a dramatic increase of phonon fluctuations and of their product far beyond the standard uncertainty principle. The inadequacy of the variational approaches was ascribed to insufficiency of the squeezed coherent phonons (harmonic oscillators) to comprise anharmonic behavior of the phonons in two-level (-band) models.

Since the early beginning,[22] Jahn-Teller model was investigated mainly in chemistry as a prototype model of electron-phonon interaction for localized centers in solids. It was used to study the instability of the orbitally degenerate electronic states of highly symmetric ionic configuration against ionic

distortions in localized molecular centers in crystals.[23,24] The effect was explained by Jahn-Teller theorem about lifting the degeneracy of an orbitally degenerate electronic state by symmetry lowering distortions of nuclear configurations. This effect is also involved, e.g., in physics of structural phase transitions in solids doped with Jahn-Teller active ions,[25] for mechanisms based on tunneling between two electronic levels coupled to phonon modes,[23] in optical[26] and paramagnetic ion spectra.[27]

Though JT effect was considered as the most representative nonadiabatic system, Born-Oppenheimer approximation has been extensively used although it is valid only in the limit of large local distortions. Inconsistency of the adiabatic approach for small distortions was analyzed by Wagner and co-workers.[23,28]

Importance of JT effect in physics was increased due to the above-mentioned discovery of JT effect based structural transitions in some high-T_c superconductors and in manganese-based perovskites. Therefore, the consideration is now focused on lattice versions of the JT model.

In this paper we will investigate an extended lattice of JT molecules: site molecules with doubly degenerate electron level coupled to two internal phonon modes with different symmetries and different coupling constants. The antisymmetric mode splits the levels, the symmetric one couples the levels via phonon assisted onsite and intersite electron transitions (Rabi oscillations). As we show, these transitions are especially important if the difference of the effective potential minima as a function of the phonon displacement is of the order of the phonon energy (symmetric Jahn-Teller molecules). We shall use a generalized variational approach which will account for *more aspects of nonadiabaticity*: Instead of simple squeezed coherent phonons, as a more appropriate variational ansatz for phonons we take a two-center-squeezed coherent wave function that accounts for the possibility of the phonon-mediated coupling of levels. The variational wave function of the two-level electron-phonon systems with reflection symmetry (antisymmetry) of the coherent phonon states related to both the levels ϕ_+ and ϕ_- was first introduced by Shore and Sander[29] as linear combinations $\phi_+ + \eta\phi_-$ and $\phi_- + \eta\phi_+$, η being new (reflection) variational parameter. The approach has been widely exploited and further developed by Wagner and co-workers[30,31] for exciton (211), dimer [(221) and (222)] systems (with the tunneling between the levels in contrast to the phonon-assisted electron transitions of our model); here the notation (xyz) is used for x as the number of the levels, y as the number of the sites, and z as the number of the electrons in a cell). The detailed comparison of the ground-state energies (GSE) of different variational phonon wave functions for an exciton-phonon or dimer-phonon models[31] confirmed the two-peak variational choice as the most suitable one, i.e., giving *the best fitting of the exact solution* in the medium- and strong-coupling regimes.

A similar structure of the wave function was proposed for the phonon wave function coupled to two electronic states of a double-well potential by Kresin and Wolf[5] in their model of the nonadiabatic origin of the isotope effect in high-T_c superconductors.

In the Sec. II, we formulate variational approach for our model. We find effective ground-state potential as a function of all (four) phonon variational parameters [displacements of two phonon modes, squeezing and reflection (mixing)].

In the Sec. III, we compare variational results for the ground-state energy of the two-center squeezed coherent phonon wave function with the adiabatic ground-state energy and identify the region of importance of the reflection (η) and nonsymmetry ($\chi=\beta/\alpha$) parameters to be the region close to $\chi=1$ ($E\otimes e$ JT symmetry). Special importance of the symmetric (Jahn-Teller) lattice molecules occurs as a specific condition for which the reflection parameter is the most effective. At this symmetry, there takes place a nonadiabatic transition between the polaron dominantly self-localized within one level, ''heavy'' polaron of a broad minimum and the almost delocalized, ''light'' polaron of a narrow minimum (with vanishing displacement) oscillating between close levels via both onsite and intersite phonon-assisted tunneling: Namely, the coherent phonons 2 are accompanied by Rabi oscillations of the electron between the levels due to the phonon mode 1. The latter virtual phonons mediate the coupling of polarons that may occupy the levels.

We compare ground-state characteristics of the ''heavy'' and ''light'' region as functions of pairs of competing classical (effective coupling) and quantum (phonon frequency, tunneling) parameters. The self-trapping due to electron-phonon coupling competes with the lattice transfer of electrons (bandwidth), which itself is being renormalized by the Debye-Waller factor. The characteristics of the related insulator-metal transition, the value of the gap and consequently of the critical coupling are determined by the complex interplay of the transfer supporting the metallic phase and of the electron-phonon coupling supporting the insulating phase. The shift of the critical line to higher values of the critical couplings due to quantum effects is discussed in the Sec. IV.

In the Sec. V we investigate anomalous behavior of the squeezed ground-state quantum fluctuations of the canonically conjugated phonon coordinates and their product on the effective coupling (μ) and effective potential asymmetry (χ) parameters, namely, the strong anharmonic fluctuations that reach their maximum values again at $\chi=1$. They decrease to the harmonic oscillator values for $\chi>1$. A related model is a lattice of two-level dimers with one spin electron at each site [(222) lattice model] studied by exact numerical methods by Borghi *et al.*[17] The present model differs from that one, but concerning the quantum fluctuations of the phonon coordinate and momenta qualitatively the same results as for their model are expected.

We remark that variational methods are widely used for electron-phonon lattice models.

A fully analytic nonvariational approach with nonconservation of the number of phonons was performed for a local ($D=0$) dimer by Weber-Milbrodt.[32] Unfortunately, in the extended ($D=1$) lattice model this method acquires extreme mathematical complexity. It was used as a basis for numerical study[16] of the above-mentioned lattice model.

II. EXTENDED (LATTICE) GENERALIZED JAHN-TELLER MODEL

We investigate 1D (one-dimensional) lattice of spinless double degenerated electron states linearly coupled to two intramolecular phonon modes described by Hamiltonian

$$H=\Omega\sum_{n,i=1,2}(b_{in}^{\dagger}b_{in}+1/2)+\sum_{n}[\alpha(b_{1n}^{\dagger}+b_{1,n})\sigma_{zn} -\beta(b_{2n}^{\dagger}+b_{2,n})\sigma_{xn}]-\frac{T}{2}\sum_{n,j=1,2}(R_{1,j}+R_{-1,j})I_n, \tag{1}$$

where $b_{i,n}, i=1,2$ are phonon annihilation operators, and the Pauli matrices σ_{ln} represent a two-level electron system. They satisfy identities $[\sigma_{ln},\sigma_{jn}]=i\sigma_{kn}$, $l=x,y,z$, representing 1/2 pseudospins related to the electron densities in a usual way, i.e., $\sigma_{xn}=\frac{1}{2}(c_{1,n}^{\dagger}c_{2,n}+c_{2,n}^{\dagger}c_{1,n})$, $\sigma_{yn}=1/2i(c_{1,n}^{\dagger}c_{2,n}-c_{2,n}^{\dagger}c_{1,n})$, $\sigma_{zn}=\frac{1}{2}(c_{1,n}^{\dagger}c_{1,n}-c_{2,n}^{\dagger}c_{2,n})$, $I_n=\frac{1}{2}(c_{1,n}^{\dagger}c_{1,n}+c_{2,n}^{\dagger}c_{2,n})$ is a unit matrix, and $c_{j,n}$ are electron annihilation operators. The operator $R_{\pm 1,j}=e^{\pm ipa}$ of the displacement by a lattice constant $\pm a$ acts in both the electron and phonon space, $R_{\pm 1,j}f_n=f_{n\pm 1}R_{\pm 1,j}$.

In terms of the creation-annihilation electron and phonon operators the Hamiltonian can be cast as follows:

$$H=\sum_{n}\left[\Omega\sum_{i=1,2}\left(b_{in}^{\dagger}b_{in}+\frac{1}{2}\right)+\frac{\alpha}{2}(n_{1n}-n_{2n})(b_{1n}^{\dagger}+b_{1n}) -\frac{\beta}{2}(c_{1n}^{\dagger}c_{2n}+c_{2n}^{\dagger}c_{1n})(b_{2n}^{\dagger}+b_{2n}) -\frac{T}{2}\sum_{j=1,2}(c_{j,n}^{\dagger}c_{j,n+1}+\text{H.c.})\right]. \tag{2}$$

For $\beta=-\alpha$, the interaction part of Eq. (1)

$$\alpha\begin{pmatrix} b_{1n}^{\dagger}+b_{1n}, & b_{2n}^{\dagger}+b_{2n} \\ b_{2n}^{\dagger}+b_{2n}, & -(b_{1n}^{\dagger}+b_{1n})\end{pmatrix} \tag{3}$$

yields the rotationally symmetric $E\otimes e$ form[24] with a pair (an antisymmetric and a symmetric under reflection) of double-degenerated vibrations. This is, e.g., the case of Cu^{++} ions with d^9 configurations in high-T_c cuprates.[33,24]

Taking $\alpha\neq\beta$ removes the degeneration of the vibronic states breaking the rotational symmetry of the electron-phonon interactions, the model still staying within the class of JT models.[1,23,22]

The dispersionless optical phonon mode b_1 splits the degenerated unperturbed electron level ($j=1,2$) while the mode b_2 mediates the electron transitions between the levels. This latter term represents phonon-assisted tunneling, a mechanism of the nonclassical (nonadiabatic) nature as well as is the pure tunneling in related exciton and dimer models.

Evidently, Hamiltonian (1) ($\alpha\neq\beta$) is reflection symmetric, $G^{(el)}G^{(ph)}H=H$,

$$|2\rangle=G^{(el)}|1\rangle,\quad (G^{(el)})^2=1,$$
$$G_{1n}^{(ph)}(b_{1n}^{\dagger}\pm b_{1n})=-(b_{1n}^{\dagger}\pm b_{1n})G_{1n}^{(ph)},\quad (G_{1n}^{(ph)})^2=1, \tag{4}$$

where $G_{1n}^{(ph)}=\exp(i\pi b_{1n}^{\dagger}b_{1n})$ is the phonon reflection operator. While the phonon 1 is antisymmetric under the reflection, phonon 2 remains symmetric.

In addition, the transfer part of Eq. (2) exhibits SU(2) symmetry of the left- and right-moving electrons (holes).

Let us note that the quantum phonon assistance of the electron tunneling [β term in Eqs. (2) and (1)] constitutes the difference of the model from the related dimer and exciton quantum models where instead of $\beta\Sigma_n(b_{2n}^{\dagger}+b_{2n})\sigma_{xn}$ of Eq. (1) there stands $\Delta\sigma_{xn}$, where Δ is the distance between the levels.[29,31]

The local part of Eq. (1) can be diagonalized in electron subspace by the Fulton-Gouterman unitary operator[34] $U_n\equiv U_{2,n}U_{1,n}$, where

$$U_{i,n}=\frac{1}{\sqrt{2}}\begin{pmatrix}1, & G_{i,n}\\ 1, & -G_{i,n}\end{pmatrix},\quad G_{i,n}=\exp(i\pi b_{in}^{\dagger}b_{in})\equiv G_{i,n}^{(ph)}, \tag{5}$$

as follows

$$\tilde{H}_L=\sum_{n}U_nH_{0n}U_n^{-1}=\Omega\sum_{n,i=1,2}\left(b_{in}^{\dagger}b_{in}+\frac{1}{2}\right) +\frac{1}{2}\sum_{n}[\alpha(b_{1n}^{\dagger}+b_{1,n})-\beta(b_{2n}^{\dagger}+b_{2n})G_{1,n})]I_n. \tag{6}$$

On the other hand, in the transfer term

$$\tilde{H}_T=-\frac{T}{2}\sum_{n}(V_{n,1}R_1+V_{n,-1}R_{-1}) \tag{7}$$

there appears a nondiagonality

$$V_{n,\pm 1}=[(1+G_{1n}G_{1n\pm 1})I_n+(1-G_{1n}G_{1,n\pm 1})G_{2n}\sigma_{zn}] \times[(1+G_{2n}G_{2n\pm 1})I_n+(1-G_{2n}G_{2,n\pm 1})\sigma_{xn}]. \tag{8}$$

Here, Pauli matrices transform as $U_i\sigma_xU_i^{-1}=G_i\sigma_z$, $U_i\sigma_zU_i^{-1}=\sigma_x$, and $U_i(b_i^{\dagger}+b_i)U_i^{-1}=(b_i^{\dagger}+b_i)2\sigma_x$.

The diagonal terms of Eq. (8) represent the polaron transfer within one level while the off-diagonal ones represent the interlevel polaron transfer through the lattice. Evidently, the contribution of the off-diagonal terms proportional to $1-G_{in}G_{i,n+1}$ is much smaller when compared with those proportional to $1+G_{in}G_{i,n+1}$.

Because of nonconservation of the number of coherent phonons, they are able even in the ground state to assist electron transitions between the levels. In the Hamiltonian (6), the operator $G_{1n}=(-1)^{b_{1n}^{\dagger}b_{1n}}$ [Eq. (5)], highly nonlinear in the phonon-1 appears mediated by phonons 2. It introduces multiple electron oscillations between the split levels mediated by *continuous virtual absorption and emission of*

the phonons 1. The effect is analogous to Rabi oscillations in quantum optics due to photons.[35] Let us note that Rabi oscillations assist both the interlevel onsite and intersite electron transitions mediated by the electron transfer T.

For various local electron-phonon models, a number of phonon variational wave functions using coherent and squeezed coherent phonons was proposed in order to reach the best ground state.[20,21,9,15]

Specially, for two-level systems Shore and Sander[29] proposed variational eigenfunctions in the form of symmetric and antisymmetric combinations of the reflection symmetric components related to both the levels. Each of these components was chosen in a form that accounted for mixing with the reflected state via new variational parameter. This choice was stated to be the best variational wave function, i.e., yielding the lowest ground-state energy. The method was further developed by Wagner and co-workers[31] for dimers and excitons. We shall adopt this approach in what follows by taking

$$\Phi_{1,2} \equiv \phi_1\psi_1 \pm \phi_2\psi_2 = \frac{1}{\sqrt{C}}[(\phi_+ + \eta\phi_-)\psi_1 \pm (\phi_- + \eta\phi_+)\psi_2] = \frac{1}{\sqrt{C}}[\phi_+(\psi_1 \pm \eta\psi_2) \pm \phi_-(\psi_2 \pm \eta\psi_1)], \tag{9}$$

with the upper sign for the ground state Φ_1 and lower sign for the excited state Φ_2.

In Eq. (9), $\phi_1 = \phi_+ + \eta\phi_-$ and $\phi_2 = \phi_- + \eta\phi_+$ are phonon wave functions related to two levels with mixing of the bare ϕ_+ (ϕ_-) and reflected ϕ_- (ϕ_+) parts mediated by the variational parameter η.

Further, ψ_1 and ψ_2 are components of the electron state vector related to the upper and lower level, respectively,

$$\psi_1(n) = c_{1n}^\dagger|0_{el}\rangle, \quad \psi_2(n) = c_{2n}^\dagger|0_{el}\rangle, \tag{10}$$

where $|0_{el}\rangle$ is the electron vacuum. Note that the last line of Eq. (9) allows us to interpret alternatively the parameter η as reflection parameter of the electron states as well.

The squeezed coherent phonon wave functions

$$\phi_\pm[\gamma_{1m}(n), \gamma_{2m}(n), r_m(n)] \equiv D_{1,\pm}[\gamma_{1m}(n)]D_2[\gamma_{2m}(n)]S_1[r_m(n)]|0_{ph}\rangle, \tag{11}$$

are related to lower (ϕ_+) and higher (ϕ_-) level; $|0_{ph}\rangle$ is the phonon vacuum.

The generators of the coherent phonons are functionals of related displacements

$$D_{1,\pm}[\gamma_{1m}(n)] = \exp\sum_m \pm[\gamma_{1m}(n)b_{1m}^\dagger - \gamma_{1m}^*(n)b_{1m}], \tag{12}$$

$$D_2[\gamma_{2m}(n)] = \exp\sum_m [\gamma_{2m}(n)b_{2m}^\dagger - \gamma_{2m}^*(n)b_{2m}], \tag{13}$$

as well as the generator of squeezing,

$$S_1[r_m(n)] = \exp\sum_m r_m(n)(b_{1m}^{\dagger 2} - b_{1m}^2). \tag{14}$$

Respective generator of the mode 2, $S_2[r_{2m}(n)] = 1$, because Hamiltonian (2) is linear in $b_2, b_2^\dagger$ and $r_{2m}(n) = 0$.

The normalization condition then reads

$$\frac{1}{N^2}\sum_{m,n} C_{1m}(n) = C, \tag{15}$$

where

$$C_{1m}(n) = 1 + \eta^2 + 2\eta\exp[-2|\tilde{\gamma}_{1m}(n)|^2], \tag{16}$$

and

$$\tilde{\gamma}_{1m}(n) \equiv \gamma_{1m}(n)\exp[-2r_m(n)]. \tag{17}$$

Generally, $\gamma_{jm}(n)$ is a nonlocal quantity that represents the displacement of the mode j at the site m due to an electron at the site n, $\gamma_{jm}(n) = 1/\sqrt{N}\Sigma_q \gamma_{jq}(n)\exp(-iqma)$. We take

$$\gamma_{jq}(n) = \frac{\gamma_j}{\sqrt{N}}\exp(iqna) \rightarrow \gamma_{jm}(n) = \gamma_j\delta_{m,n}, \tag{18}$$

where γ_j are independent of n. Equation (18) indicates that the phonon displacement accompanies the electron at the site n. The same is valid for the squeezing, $r_m(n) = r\delta_{m,n}$.

Full Bloch solution to the transformed lattice Hamiltonian $\tilde{H} = \tilde{H}_L + \tilde{H}_T$, [Eqs. (6), (7)] is chosen as a generalized Fulton-Gouterman variational ansatz[34,31] in the vector form [Eq. (9)],

$$\Psi_{FG}(k) = \frac{1}{\sqrt{C}}\sum_n \exp(ikna)\begin{pmatrix}\phi_1(n)\psi_1(n)\\ \phi_2(n)\psi_2(n)\end{pmatrix}, \tag{19}$$

where the electron parts ψ_i are defined by Eq. (10) and the phonon parts $\phi_i(n)$ by Eqs. (9) and (11)–(14).

We have investigated the model (2) in a former paper[36] with respect to the stability of a soliton ground state against quantum fluctuations. However, the variational wave function we used did not account for the two-center nature of the wave function here respected by the reflection parameter η [Eq. (9)].

In what follows the ground-state energy as a function of the optimized variational parameters η, γ_1, γ_2, r will be determined.

III. THE GROUND STATE

When considering the ground state of $\tilde{H} = \tilde{H}_L + \tilde{H}_T$, [Eqs. (6) and (7)], we omit the electron and phonon dynamic terms by setting $k = 0, q = 0$.

By averaging $\tilde{H} = \tilde{H}_L + \tilde{H}_T$ [Eqs. (6), (7)] over the phonon wave functions (19) with (9) and (11) one obtains for the site Hamiltonian (6) (Appendix B)

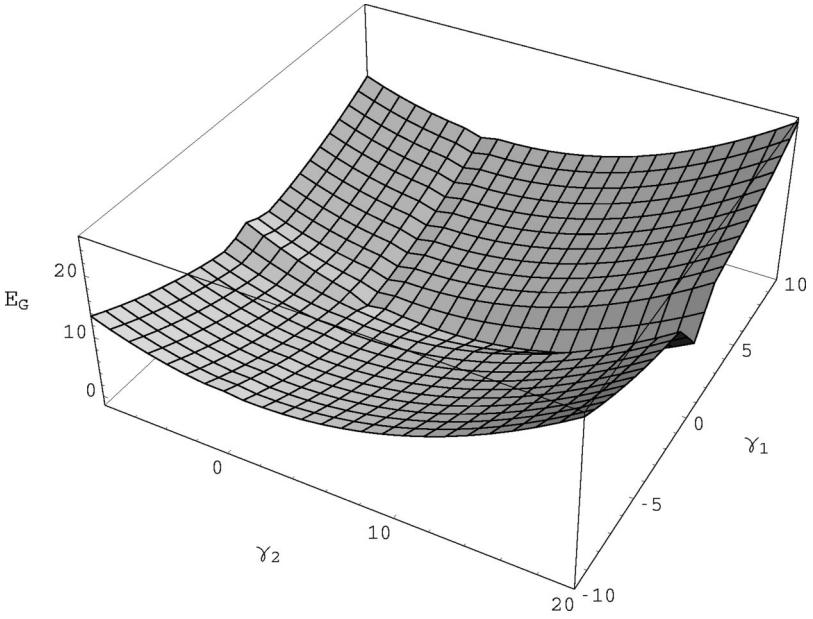

FIG. 1. The potential (20) for $\chi=\beta/\alpha=0.5$, $\mu=2$, $\Omega=0.05$ and $T=1$ as function of γ_1,γ_2.

$$\frac{\langle \tilde{H}_L \rangle}{N} \equiv H_{ph} + H_{int}, \tag{20}$$

where

$$H_{ph} = \frac{\Omega}{2}(\cosh 4r + 1)I + \Omega \frac{1+\eta^2-2\eta e^{-8r_1}\exp(-2|\tilde{\gamma}_1|^2)}{1+\eta^2+2\eta\exp(-2|\tilde{\gamma}_1|^2)}|\gamma_1|^2 I + \Omega|\gamma_2|^2 I, \tag{21}$$

$$H_{int} \equiv H_\alpha + H_\beta = \frac{\alpha(1-\eta^2)}{1+\eta^2+2\eta\exp(-2|\tilde{\gamma}_1|^2)}\gamma_1\sigma_z - \frac{\beta[(1+\eta^2)\exp(-2|\tilde{\gamma}_{1q}|^2)+2\eta]}{1+\eta^2+2\eta\exp(-2|\tilde{\gamma}_1|^2)}\gamma_2 I, \tag{22}$$

where H_α and H_β are α- and β-dependent parts of the interaction H_{int} [Eq. (22)]. From the transfer Hamiltonian $\tilde{H}_T$ (7) there remains

$$\frac{\langle \tilde{H}_T \rangle}{N} = -T\exp(-W)M \equiv 2(H_{T1}I + H_{T2}i\sigma_y + H_{T3}\sigma_z + H_{T4}\sigma_x). \tag{23}$$

The Debye-Waller factor $\exp(-W)M$ in Eq. (23) is given in the Appendix B. The differential part of the Debye-Waller factor W in the ground state is zero. For M it holds

$$M = [(1+E_1^2)I + (1-E_1^2)E_2\sigma_{zn}][(1+E_2^2)I + (1-E_2^2)\sigma_x], \tag{24}$$

where E_i are given by (Appendix B)

$$E_1 \equiv \exp(-2|\tilde{\gamma}_1|^2), \quad E_2 \equiv \exp(-2|\gamma_2|^2). \tag{25}$$

Expressions E_i [Eq. (25)] in the ground state are independent of q and n because of the form of $\gamma_{iq}(n)=\gamma_i\exp(-iqna)$ [Eq. (18)]. This substantially simplifies subsequent calculations leaving E_i and C_1 as functions of γ_i^2 independent on n. The transfer terms $H_{Ti}, i=1,2,3,4$ in Eq. (23) with Eq. (24) are expressed as

$$\begin{aligned} H_{T1} &= -\frac{T}{4}(1+E_1^2)(1+E_2^2), \\ H_{T2} &= -\frac{T}{4}(1-E_1^2)(1-E_2^2)E_2, \\ H_{T3} &= -\frac{T}{4}(1-E_1^2)(1+E_2^2)E_2, \\ H_{T4} &= -\frac{T}{4}(1+E_1^2)(1-E_2^2). \end{aligned} \tag{26}$$

Here, H_{T1}, H_{T3} and H_{T2}, H_{T4} are diagonal and off-diagonal terms of Eq. (23), respectively.

The effective polaron potential in Eq. (20) [with Eqs. (21)–(25)] as a highly nonlinear function of γ_1 and γ_2 is visualized in Fig. 1.

The potential exhibits two sets of minima related to two competing ground states:

(i) Two nonequivalent broad minima related to both the levels (12) at $\pm\gamma_1 \neq 0$ and γ_2 close to 0;

(ii) One narrow minimum at γ_1 close to 0, $\gamma_2 > 0$, where both levels approach close together. This minimum develops at growing β; evidently its behavior depends also on T value because of nonlinearity of the Debye-Waller factor M [Eqs. (24) and (25)].

The ground-state energies related to these two sets of competing minima were calculated numerically. The result of the numerical minimization of the diagonalized form of energy (20),

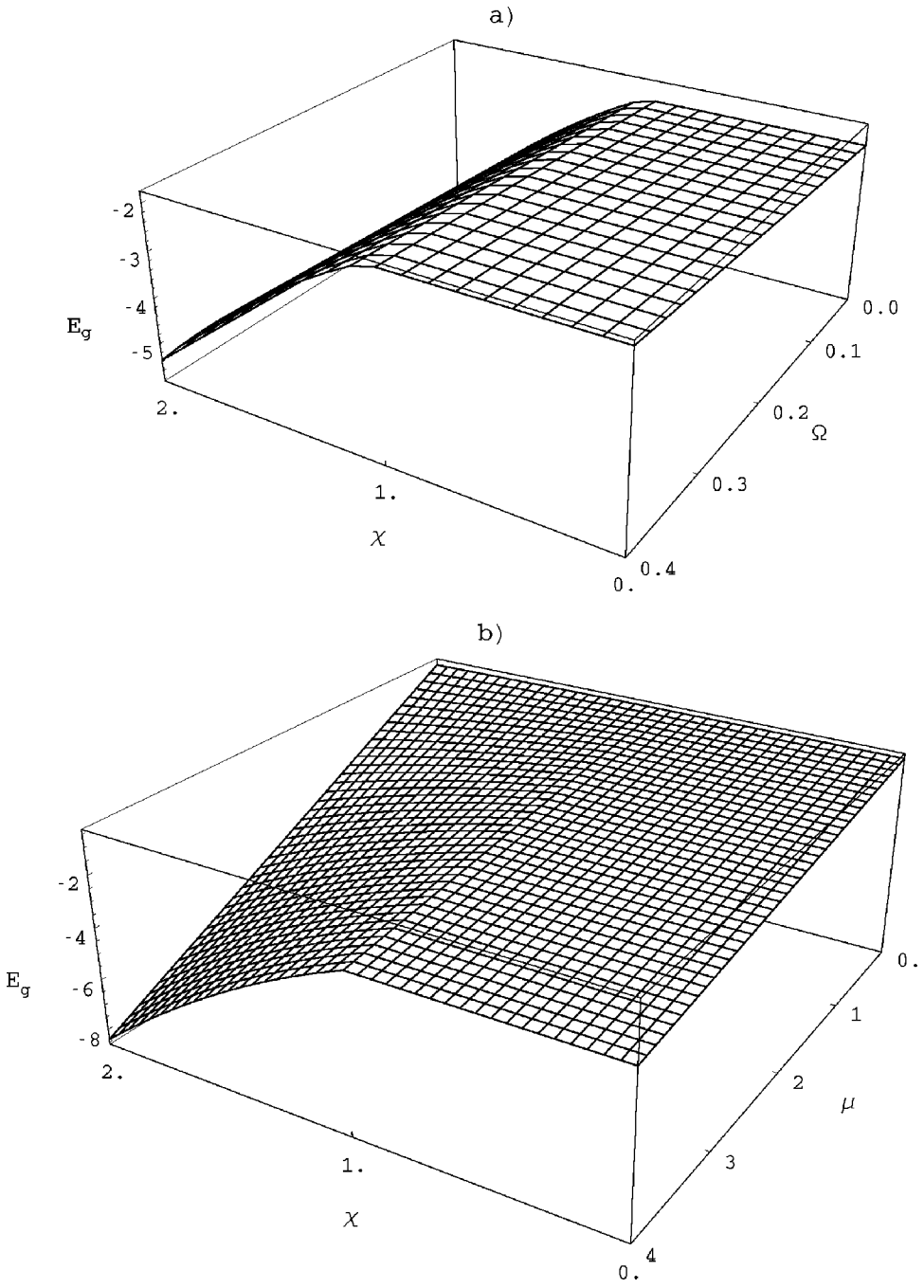

FIG. 2. The ground-state energy (28) in the χ-Ω plane at $\mu=2.5$ (a) and (b) in the χ-μ plane at $\Omega=0.5$. The ''light'' phase is evidently much more sensitive to effects of χ and μ than the ''heavy'' polaron.

$$E=H_{ph}+H_{\beta}+H_{T_1}-[(H_{\alpha}+H_{T_3})^2+H_{T_4}^2-H_{T_2}^2]^{1/2} \tag{27}$$

can be written symbolically as

$$E_G(\mu,\chi,\Omega/T)=E(\{\gamma_{1q},\gamma_{2q},r,\eta\}_{min})/T. \tag{28}$$

Here, the index *''min''* denotes the optimized values. The model parameters

$$\mu=\frac{\alpha^2}{2\Omega T},\quad \chi=\frac{\beta}{\alpha},\quad \frac{\Omega}{T} \tag{29}$$

are parameters of the effective interaction, asymmetry, and nonadiabaticity, respectively. Energy E_G [Eq. (28)] is in scaled units, renormalized by T. The results of the numerical evaluations of the ground-state energy (28) are depicted in Figs. 2(a) and 2(b) for different model parameters.

One can distinguish there two regions depending on the value of χ with different behavior of ground state in each of them:

(i) The ground state pertaining to the lower broad minimum at $\gamma_1<0$ and $\gamma_2\approx 0$ with a small reflection part at $\gamma_1>0$ is referred to as a ''heavy'' region. It corresponds to a predominantly intralevel ''heavy'' polaron that is represented by a two-peak wave function, both peaks representing a harmonic oscillator ($\sim\exp[-(x\mp\gamma_1)^2]$) displaced by the value $\pm\gamma_1$ [as it is seen from the form of the ansatz (12)]. The

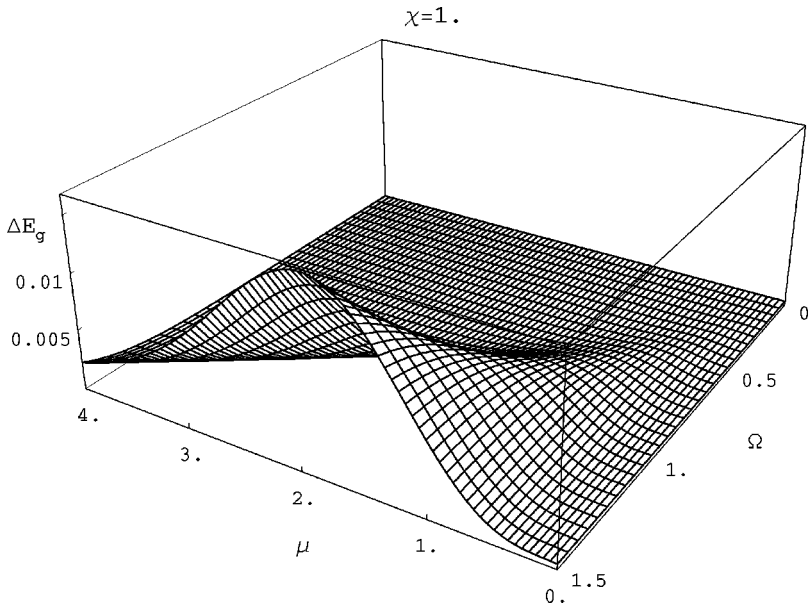

FIG. 3. The range of relevance of the reflection measure η: Difference $\Delta E_G = E_G(\eta=0, r=0) - E_G$, for $\chi=1$, E_G is the exact ground state (28). For $\chi<1$, the difference increases with χ reaching its maximum at $\chi=1$. At $\chi>1$ it drops to zero, i.e., the narrow minimum "light" phase is resistant against η.

"heavy" polaron is dominant at $\chi<1$ where the broad minimum $\gamma_1<0$ is dominating.

(ii) Close to $\chi=1$, the energies of two minima go very close together (their difference is in the order of the phonon energy Ω). They drop to one narrow minimum that represents a new ground state. *Close to* $\chi=1$, *continuous transition to a new ground state occurs*. It stabilizes at $\chi>1$, where (optimized) γ_1 value is close to 0 and $\gamma_2>0$. This region is referred to as a "light" polaron region because, owing to the abrupt decrease of $\gamma_1 \approx 0$ at $\chi>1$, the effective mass of the intralevel polaron drops to almost its free-electron value, i.e., *the polaron self-localization vanishes in the "light" region*. Because of this "undressing," the transport characteristics of the excited electron would increase. Moreover, due to the tiny distance between the levels, their coupling takes place by the exchange of virtual phonons 1. At suitable conditions, in the excited state, when both levels are occupied by electrons of opposite spins, *the mechanism of virtual phonon exchange implies the pairing of electrons*, i.e., *formation of "light" bipolarons*.

The ground-state energy, especially its behavior dependent on pairs of parameters χ, Ω and χ, μ is illustrated in details in Fig. 2. While being weakly Ω dependent, the energy strongly decreases with χ inside the "light" phase [Fig. 2(a)]. The position of the phase line is slightly shifted from $\chi=1$ at $\Omega=0$ to higher values of χ with increasing Ω. This is consistent with the fact that the phonon fluctuations are most effective when the difference between the energies of the phases is of the order of the phonon energy.

The ground-state energy in the "heavy" region ($\chi<1$) is independent of χ, its decrease inside the "light" region ($\chi>1$) is dependent on the effective coupling μ [Fig. 2(b)]. The energy decrease due to μ is stronger in the "light" phase (depending on χ) than in the "heavy" phase.

The region of importance of reflection measure η and r is illustrated in the Fig. 3. There we show the difference between the ground-state energy with r and η omitted and ground state with four variational parameters calculated numerically. However, contribution due to $r\, E_G(\eta, r=0) - E_G \sim 2\times 10^{-3}$ of the maximum value in Fig. 3. The said parameters turn out to be most relevant in $E\otimes e$ JT case ($\chi=1$).

The effects of η and r on the ground state is apparent only at moderate couplings in the "heavy" region, reaching their maximum at $\chi=1$. The narrow minimum (the "light" region) is resistant against η.

In order to demonstrate important properties of displacements (μ and Ω dependence) it is sufficient, except for the region of importance of the reflection (Fig. 3) inside the "heavy" region apparent for γ_2 (Fig. 4), to calculate them in the limit $\eta=0$. We shall use Eq. (27) approximated for the cases of both "heavy" and "light" polarons and obtain implicit expressions for γ_i that, however, are good to visualize their behavior in both regions:

(i) "heavy" polaron (γ_2 small, $E_2 \approx 1, H_{T_2}, H_{T_4} \approx 0$):

$$\gamma_1 \approx \frac{-\alpha e^{4r}}{2TE_1^2\left[2+\dfrac{\Omega e^{4r}}{TE_1^2}\right]}, \tag{30}$$

γ_2 is small except for the region of fluctuations visualized in Fig. 4. One can see, that the self-localization due to phonons 2 in the "heavy" region $\sim -\gamma_2^2$ clearly implies the "cave" in the ground-state energy due to the reflection measure η (anharmonicity) of the ground state (Fig. 3).

(ii) "light" polaron (γ_1 small, $E_1 \approx 1, H_{T_2}, H_{T_3} \approx 0$):

$$\gamma_1 \approx \frac{-\alpha e^{4r}}{2TE_1^2\left(1+\dfrac{\beta^2}{2\Omega T}+\dfrac{\Omega e^{4r}}{TE_1^2}\right)} \approx 10^{-8},$$
$$\gamma_2 \approx \frac{\beta}{2TE_2^2\left(2+\dfrac{\Omega}{TE_2^2}\right)}. \tag{31}$$

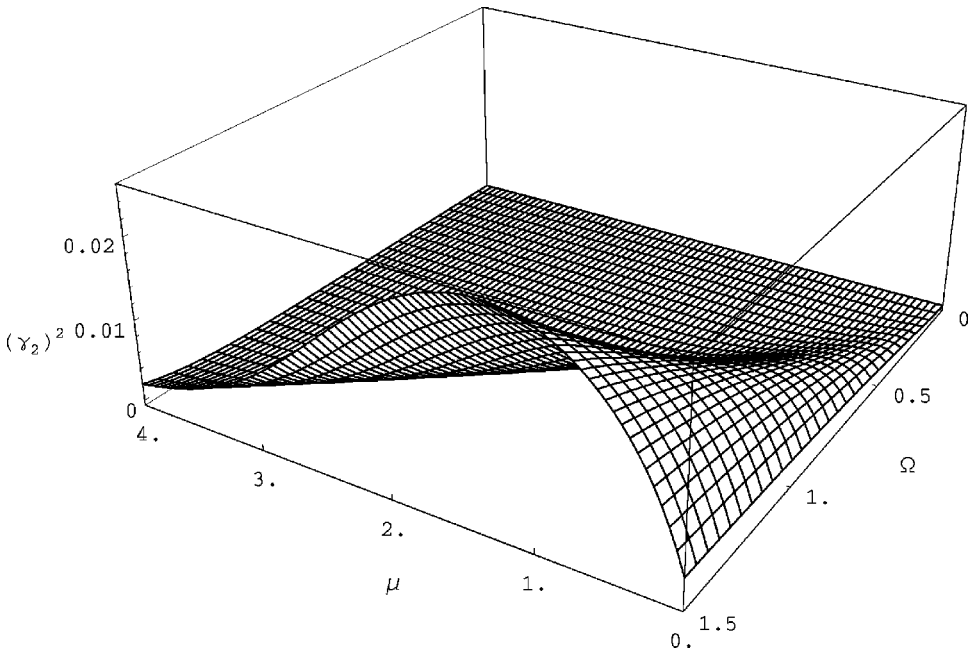

FIG. 4. Displacement γ_2^2 of phonons 2 in the ''heavy'' region ($\chi=1$); it evidently implies the ''cave'' due to reflection η of the ground-state energy in the ''heavy'' region (Fig. 3).

In the ''light'' region the fluctuations of γ_1 are missing as well as the fluctuations of the energy. This is consistent with the above result of the resistance of the narrow minimum against η.

For both ''heavy'' and ''light'' polaron a dependence of γ_i on the nonadiabaticity parameter Ω/T appears. It implies the dependence of the Debye-Waller factor and consequently of the polaron mass on the phonon frequency Ω. This can be thought of as an analogy of the *isotope effect* at zero temperature.

In the ''heavy'' phase, electron transitions mediated by phonons 2 to the upper level enhance fluctuations $\sim\gamma_2$, which mix phonons 2 with phonons 1 and contribute to the fluctuations of the ground-state energy of the heavy region. This is the reason for the similarity of the results in Figs. 3 and 4.

IV. METAL-INSULATOR TRANSITION

To illustrate the effect of various interactions, let us consider first a simple two-level case ($T=0$). The ground state will be obtained by the numerical minimization of energy

$$E^0=H_{ph}+H_\alpha+H_\beta, \tag{32}$$

where H_α and H_β are α- and β-dependent components of the interaction term H_{int} [Eq. (22)]. The result is of the form

$$E_G^0=\frac{\Omega}{2}(\cosh 4r^0+1)-H_{P\alpha}-H_{P\beta}, \tag{33}$$

where the label 0 specifies the optimized variational values. In Eq. (33), $H_{P\alpha}$ and $H_{P\beta}$ are contributions of the self-localization energies of two coupled polarons proportional to $\alpha^2/2\Omega$ and $\beta^2/2\Omega$, respectively. The splitting of the levels is implied to be

$$\Delta^0=2|E_G^0|. \tag{34}$$

Correspondingly, a lattice of JT molecules ($T\neq 0$) shows either metallic or insulating phase behavior depending on whether the split bands overlap or not. Usually the resulting situation depends strongly on the phonon renormalization of the gap and of the electron band including phonon fluctuations.

Our aim here is to investigate the metal-insulator transition due to the competition of the polaron localization and the delocalization due to the transfer including the phonon-assisted electron transfer effects. Namely, the transport terms H_{Ti} compete the level splitting (34) because of the complex interplay of the diagonal and off-diagonal contributions to the bandwidth. In order to find the value of the gap as an order parameter of the metal-insulator phase transition it is necessary to perform usual renormalization: SU(2) symmetry of the right- and left-moving electrons and holes of the transfer part of Hamiltonian (1) makes it possible to split electron operators onto an electron and a hole part,

$$c_i=c_{i,+}+c_{i,-}, \quad i=1,2, \tag{35}$$

the signs $\pm$ indicating directions of the electron motion. In view of the reflection symmetry of the two-level local part of Hamiltonian (1) against the level $E=0$ in the middle between the levels electron operators (35) can be rewritten in a renormalized form,

$$c_1=c_{1,+}^{(el)}+c_{1,+}^{(h)\dagger}, \quad c_2=c_{2,-}^{(h)\dagger}+c_{2,-}^{(el)}. \tag{36}$$

This renormalization implies the change of the sign of T (H_{T_i}) for holes ($E<0$).

There are two pairs of electrons and holes, $c_{1,+}^{(el)}$, $c_{2,-}^{(h)\dagger}$ and $c_{2,-}^{(e)}$, $c_{1,+}^{(h)\dagger}$, i.e., two state vectors $\binom{f_+}{g_-^*}$ and $\binom{-g_-}{f_+^*}$, which satisfy equations

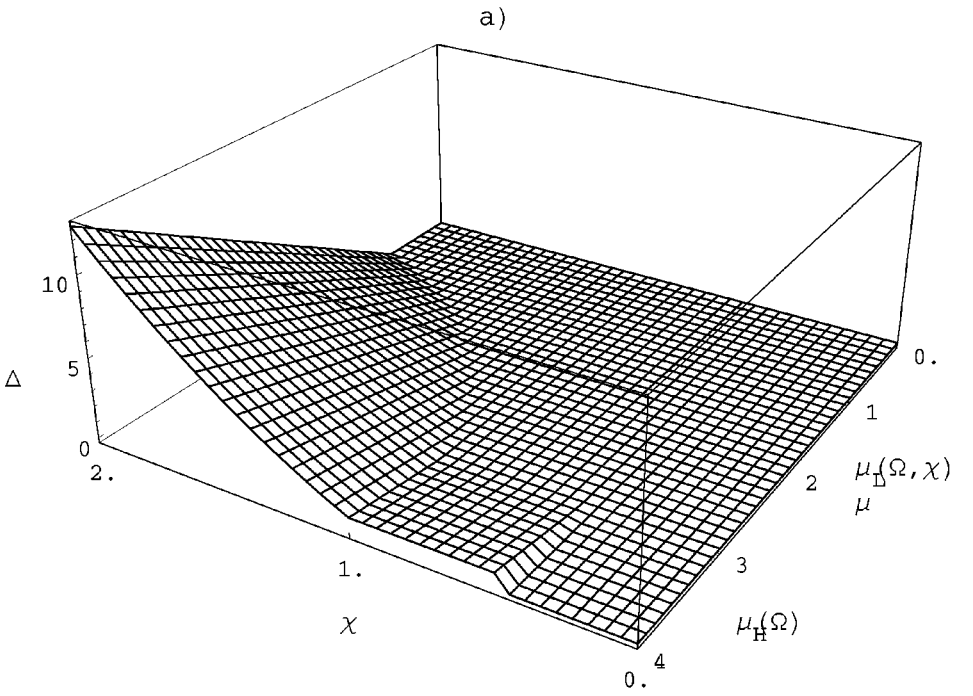

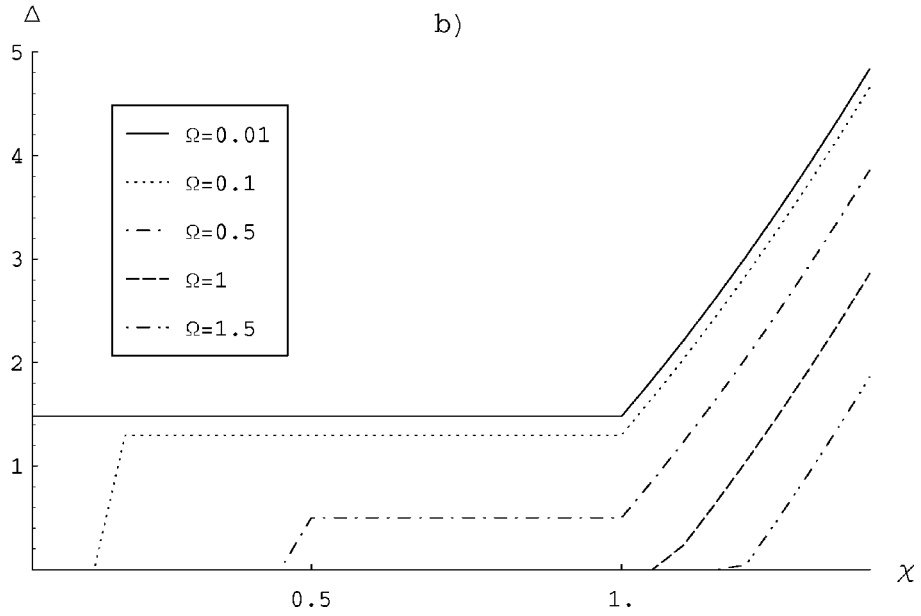

FIG. 5. (a) The gap in the plane of μ and χ for $\Omega=0.5$. While the critical coupling $\mu_H(\Omega)$ for *I-M* transition in the "heavy" phase ($\chi<1$) is very slightly dependent of χ, $\mu_L(\Omega,\chi)$ in the "light" phase refers to the transition curve for $\chi>1$. (b) The shift of the metal-insulator transition in the "heavy" region due to quantum fluctuations at strong coupling $[\mu>\mu_H(\Omega)]$.

$$H_m\begin{pmatrix} f_+ \\ g_-^* \end{pmatrix}+\begin{pmatrix} -\Delta/2, & 0 \\ 0, & \Delta/2 \end{pmatrix}\begin{pmatrix} -g_-^* \\ f_+ \end{pmatrix}=0, \tag{37}$$

$$H_m\begin{pmatrix} -g_- \\ f_+^* \end{pmatrix}+\begin{pmatrix} \Delta/2, & 0 \\ 0, & -\Delta/2 \end{pmatrix}\begin{pmatrix} f_+^* \\ g_- \end{pmatrix}=0, \tag{38}$$

where H_m results from the minimization of Eq. (20) with respect to the variational parameters (28),

$$H_m=\begin{pmatrix} -E_G, & 0 \\ 0, & E_G \end{pmatrix}, \tag{39}$$

and E_G given by Eq. (28).

The solution for the gap Δ finally reads [see Figs. 2(b)–4(b)]

$$\Delta=2|E_G(T\to -T)| \tag{40}$$

and implies a condition for the stability of either the insulating phase, if $E_G(T\to -T)>0$, or the metallic phase in the opposite case, where $\Delta\equiv 0$.

Figure 5 depicts both *I-M* and "heavy"-"light" transitions. In the "heavy" phase, at small Ω the *I-M* transition line is determined by the critical coupling $\mu_H(\Omega)$ independent of χ up to $\chi=1$. In the "light" phase, the critical coupling $\mu_L(\Omega,\chi)<\mu_H(\Omega)$ decreases with increasing χ. The point $[\chi=1,\mu_H(\Omega)]$ is the only point of coincidence of the

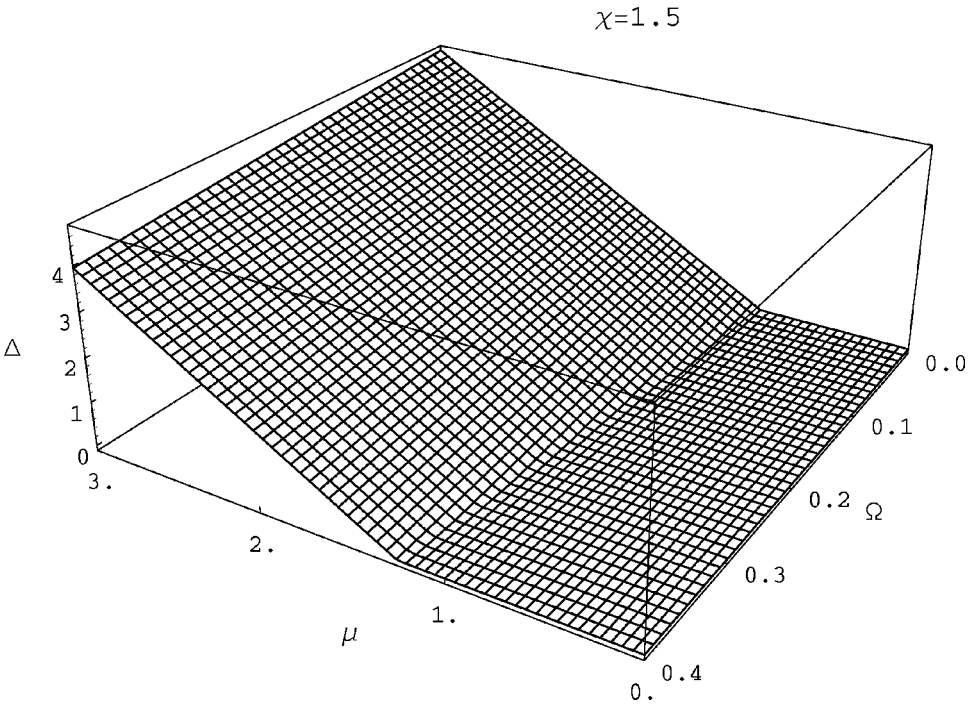

FIG. 6. The gap in the "light" region ($\chi>1$) as a function of Ω and μ for $\chi=1.5$. The fluctuations increase with Ω.

"heavy"-"light" transition and the *I-M* transition. At small μ the fluctuations support the metallic phase in the light region [Fig. 5(a)], while at small χ (and sufficiently large μ that the insulating phase could be stable) they support the metallic phase in the heavy region [Figs. 5(a,b)].

The *I-M* transition can appear in the "heavy" region at large μ (29) and small Ω [Fig. 2(a)]. From Fig. 3 (medium values of μ) one can locate the region of relevant reflection η into the metallic phase, where the bands overlap. The "light" region ($\chi>1$) is resistant against η: no similar effect as that one shown in Fig. 3 there exists. Therefore, in the heavy region the metallic phase is strongly supported due to the fluctuations at weak couplings μ. Heavy phase is therefore metallic in the broad range of parameters except for strong couplings [Fig. 2(b)]. At certain (large) μ the *I-M* transition drops close to the line $\chi=1$, so that the transition coincides with the heavy to light polaron transition. With decreasing μ the *I-M* transition line moves to larger χ [Fig. 5(b)]: the *M-I* transition moves away from the heavy-light transition into the light region. In the light region the *I-M* transition line moves to smaller μ when compared with the heavy region (Fig. 6).

As one can also see from Figs. 6 and 8, the *I-M* transition line in the phase diagram μ,Ω is strongly Ω dependent. The phase line in the plane (μ,Ω) between the phases shows the broadening of the metallic phase with growing Ω, i.e., the metallic phase is supported by the quantum fluctuations. Respective ground-state energy slightly increases with Ω.

To make effects of different contributions H_{T_i} more transparent, we can first analytically calculate the effect of the diagonal terms H_{T_1} and H_{T_3}. [Let us note that neglecting the off-diagonal transfer, i.e., H_{T_i}, $i=2,4$ in Eq. (26), means neglecting the additional splitting of the bands. More precisely, it means neglecting the off-diagonal terms in Eq. (8)].

Minimization of the energy (27) with $H_{T_2}=H_{T_4}=0$,

$$E^1=H_{ph}+H_\alpha+H_\beta+H_{T_1}+H_{T_3}, \tag{41}$$

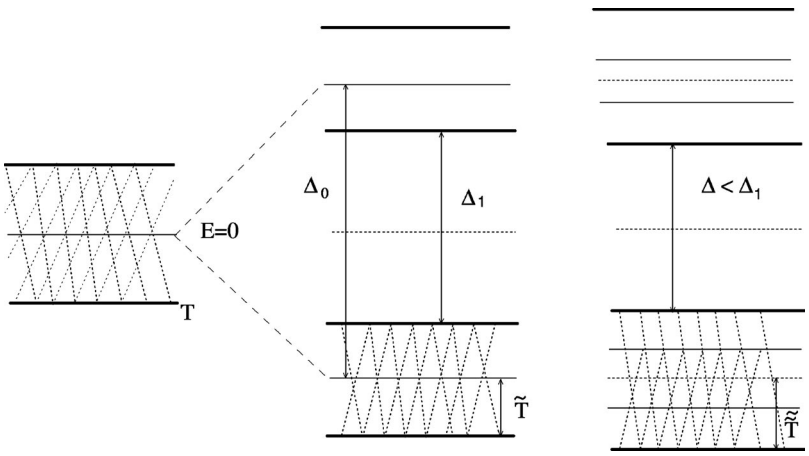

FIG. 7. The competition of the level splitting and bandwidth T terms [$\tilde{T}=TM$ (23)]. Δ_0 is splitting of the levels (34), Δ_1 neglects the off-diagonal terms H_{T_2},H_{T_4}, [Eq. (43)]. Δ is the exact gap given by Eq. (40).

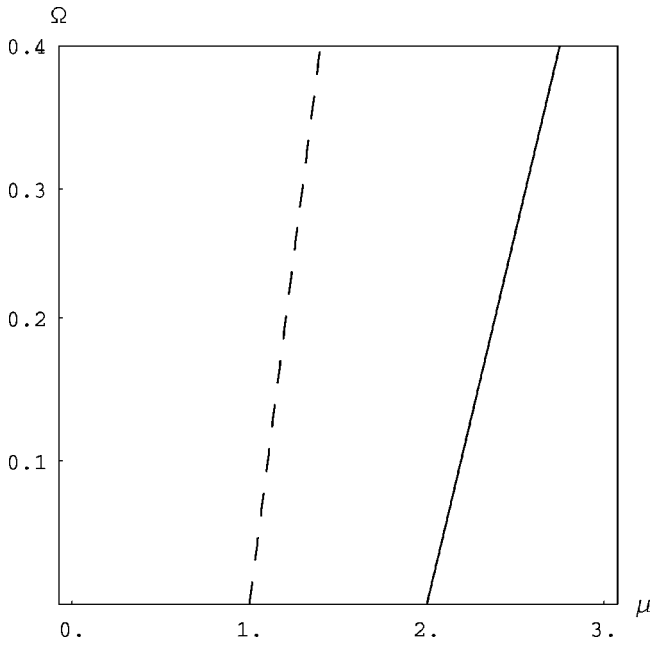

FIG. 8. Comparison of the phase diagram of the exact model (40) (solid line) with that one neglecting off-diagonal transfer (43) (dashed line) of the heavy region. The metallic phase occurs on the left and the insulator on the right of the respective line.

implies the ground state of a similar structure as that one of Eq. (33),

$$E_G^1=\frac{\Omega}{2}(\cosh 4r^1+1)-H_{P\alpha}^1-H_{P\beta}^1+H_{T_1}^1+H_{T_3}^1, \quad (42)$$

where the label 1 specifies the optimized variational values. Respective splitting yields

$$\Delta^1=2|E_G^1-2(H_{T_1}^1+H_{T_3}^1)|$$
$$=2|H_\Omega^1-H_{P\alpha}^1-H_{P\beta}^1-H_{T_1}^1-H_{T_3}^1|. \quad (43)$$

The qualitative picture of the role of different contributions in the formation of the gap is given in Fig. 7.

The exact phase diagram is compared with the result of Eq. (43) in Fig. 8. Here one can see that the main contribution to the shift of the phase diagram in support of the metallic phase is on account of the off-diagonal electron transfer terms H_{T_2} and H_{T_4} (26) related to phonon assisted Rabi oscillations. These contributions play an important role in the light phase [Fig. 2(b)].

V. SQUEEZED QUANTUM GROUND STATE (VACUUM) FLUCTUATIONS OF PHONONS

In Fig. 9 we display numerical results for the coordinate and momentum fluctuations of the phonon in the heavy region ($\chi<1$) of the ground state. Evident anharmonicity

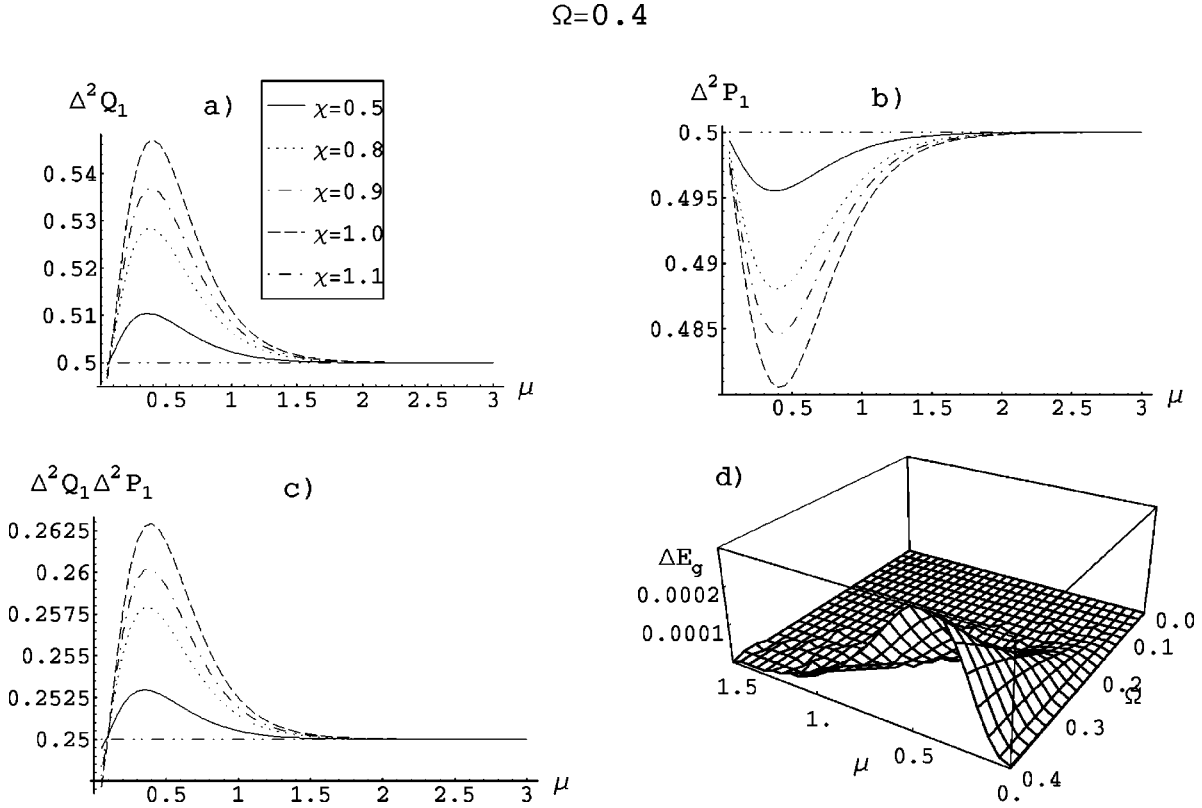

FIG. 9. Quantum fluctuations of (a) the coordinate $\Delta^2 Q_1$, (b) momentum, $\Delta^2 P_1$ and (c) their product $\Delta^2 Q_1 \Delta^2 P_1$. (d) Details of Fig. 3 underlying the region of parameters of Figs. 9(a–c).

peaks in the region of relevance of the reflection η [Fig. 9(c)] are due to the mixing with the phonon of the higher level. The peaks are related to the ground-state (squeezed vacuum) fluctuations of the phonon coordinate $Q_1 = 1/\sqrt{2}(b_1^\dagger + b_1)$,

$$\Delta^2 Q_1 = \langle Q_1^2 \rangle - \langle Q_1 \rangle^2 = \frac{1}{2}\exp(4r)\left[1 + 4\tilde{\gamma}_1^2 - \frac{4(1-\eta^2)^2\tilde{\gamma}_1^2}{[1+\eta^2+2\eta\exp(-2\tilde{\gamma}_1^2)]^2}\right], \tag{44}$$

$\tilde{\gamma}_1$ defined by Eq. (17). For the variational parameters γ_1, η, r we have to take their optimized (ground state) values. For the related momentum $P_1 = (i/\sqrt{2})(b_1^\dagger - b_1)$, one obtains the ground-state fluctuation

$$\Delta^2 P_1 = \langle P_1^2 \rangle - \langle P_1 \rangle^2 = \frac{1}{2}\exp(-4r), \tag{45}$$

where again the optimized value for r is meant.

Their product $\Delta^2 Q_1 \Delta^2 P_1$ for the oscillator in the ground state [Fig. 9(c)] exhibiting a peak in the region of relevant reflection η is the evidence for its anharmonicity due to the coupling with the higher-level oscillator. The reflection variational parameter η is efficient only in the heavy region ($\chi < 1$), for $\chi = 1$ the fluctuations decrease close towards the classical value 0.25 of the harmonic oscillator near the narrow minimum: the stable ground state of the light polaron is achieved at $\chi = 1$. In the light region the oscillator remains close to harmonic one; no analogous effects to those in the heavy region occur. The results displayed in Fig. 9 stay in evident correlation with the region of relevance of the reflection parameter η of the Fig. 3 (see its detail in Fig. 9(d) for the corresponding region of parameters). Similar effects of anharmonicity were found by numerical simulations in the related model by Borghi *et al.*[16] mentioned in the Introduction.

VI. CONCLUSIONS

The self-consistent polaron potential provided by the Holstein intralevel and interlevel electron-phonon couplings in our two-level lattice model is highly nonlinear function of phonon displacements (Fig. 1). As a consequence, there occurs a competition between the regime of two nonequivalent broad minima at $\pm\gamma_1$ and γ_2 close to 0 related to two electron levels and the regime of one narrow minimum at $\gamma_2 > 0$ and γ_1 close to 0 when both broad minima collapse to a single one, so that both levels drop to that minimum. The broad minima dominate at $\chi < 1$, the narrow one at $\chi > 1$. At $E \otimes e$ Jahn-Teller symmetry ($\chi = 1$) energies of the broad and narrow minima coincide and the phonon-assisted tunneling due to the nonadiabatic fluctuations reaches its maximum close to this limit. When χ is approaching 1, there occurs pairing of the levels due to the interlevel onsite and intersite polaron tunneling mediated by the exchange of virtual phonons. The narrow minimum is suppressed if the electron transfer energy T decreases.

Hence, we have identified two regions of stability: (i) the region of the dominating *heavy polaron* ($\chi < 1$) related to the broad minimum at negative γ_1 (the absolute minimum) and $\gamma_2 \approx 0$ and (ii) the region of the dominating *light polaron* ($\chi > 1$) related to the narrow minimum at $\gamma_1 \approx 0$ (Fig. 1). The almost *vanishing polaron self-localization* in the ''light region'' (''undressing'') means *enhancement of the polaron transfer* due to respective decrease of the polaron effective mass. Even in the heavy phase the effect can be present due to fluctuations of the light phase (Figs. 3 and 4).

Close to the transition from heavy to light polaron at $\chi = 1$, a continuous transition to *new ground state that is stable at* $\chi > 1$ *occurs* (Fig. 2). In this ground state the *formation of light bipolarons* is possible, which are characterized by the enhancement of the effective transfer due to the vanishing self-localization. The pairing of the polarons is caused by virtual exchange of phonons 1 mediated by phonons 2 between the electrons in both levels at suitable configuration. This effect might be of interest from the point of view of bipolaron mechanisms of the superconductivity.[12] The *I-M* transition and heavy-light phase coincide in the crossing point of the lines $\chi = 1$ and $\mu_H(\Omega)$ [critical line of *I-M* transition in the heavy phase, Fig. 5(a)].

The Debye-Waller factor (24) shows nonadiabatic dependence on the phonon frequency Ω through γ_i, [Eqs. (30), (31)]. Then, the effective transfer parameter of electrons is correspondingly increased and the electron effective mass decreased. This effect reminds us of the ''isotope effect,'' however, at zero temperature.

The metal-insulator transition occurs in both regions: heavy region is the region of dominating metallic phase, where the transition to the insulating phase can occur only at sufficiently large μ (Fig. 5). On the other hand, in the light region the *I-M* transition can occur at relatively small μ (Figs. 5 and 6). For certain μ the *I-M transition can coincide with the heavy-light polaron transition* at $\chi = 1$ [Fig. 5(a)]. The interlevel and the combined interlevel and intersite electron Rabi oscillations in the ground state, are identified to be the main reason for the *shift of the I-M transition line to stronger effective couplings*, i.e., *in support of the metallic phase* (Figs. 5 and 7). Figure 5(a) illustrates the existence of the light polaron in both the insulating and metallic phase.

Fluctuations of the phonon-conjugated coordinates and their product exhibit peaks (Fig. 9) in the region of parameters where the effect of η (Figs. 3, 4) is relevant. Consequently, the effect appears only *in the heavy region* reaching its maximum at $\chi = 1$ and growing with Ω. The peaks are evidence for *the strongly anharmonic behavior* of the heavy polaron in the region of relevance of η. In the light region, there occurs a degeneracy over η (no effect of η on the minimum of the potential), i.e., no analogous effect of the fluctuations, but nearly a harmonic oscillator is observed. This is obviously due to the specific form of the variational ansatz, which is inspired by the shape of the ''pure'' heavy polaron (i.e., with $\chi \ll 1$). Therefore the ansatz (9), reflecting the essentials of the heavy polaron, is proper for describing the heavy region, but when concerning the light region, it presents, to some extent, a heuristic extrapolation. We could have started from another ansatz underlying the essentials of light polaron (which could be, for example, inspired for the

''pure'' case of $\chi \gg 1$) in order to investigate the light region and gain some extrapolation towards smaller χ. Naturally, the transition $E \otimes e$ Jahn-Teller case ($\chi \simeq 1$) too needs further considerations.

ACKNOWLEDGMENTS

We thank Professor M. Wagner for useful discussions and Professor J. Peřina for careful reading of the manuscript. The support from the Grant Agency of the Czech Republic (Grant No. 202/01/1450) and partly also from the VEGA (Grant No. 2/7174/20) is highly acknowledged.

APPENDIX A

We shall use the following formulas[37,38]

$$D(\gamma)S(r)=S(r)D(\tilde{\gamma}), \quad \tilde{\gamma}=\gamma e^{-2r}, \tag{A1}$$

$$S^{-1}(r)bS(r)=b\cosh 2r+b^{\dagger}\sinh 2r, \tag{A2}$$

$$\langle 0|S^{-1}[r_m(n)]D^{-1}[\gamma_m(n)]D_m(n+1)S[r_m(n+1)] = \exp(-\tfrac{1}{2}[\tilde{\gamma}_m(n+1)-\tilde{\gamma}(n)]^2), \tag{A3}$$

where $\tilde{\gamma}=\gamma e^{-2r}$.

For averages obtained by using virtual Fock states $|n\rangle$, we use formulas

$$\langle 0|D^{-1}S^{-1}(-1)^{b^{\dagger}b}SD|0\rangle \equiv {}_g\langle\gamma|(-1)^{b^{\dagger}b}|\gamma\rangle_g=\sum_{n=0}^{\infty}(-1)^n|\langle n|\gamma\rangle|^2, \tag{A4}$$

where $|\gamma\rangle_g=SD|0\rangle=S|\gamma\rangle$ and,

$$\langle n|\gamma\rangle_g=\frac{1}{(n!\mu)^{1/2}}\left(\frac{\nu}{2\mu}\right)^{n/2}H_n\left(\frac{\gamma}{(2\mu\nu)^{1/2}}\right)\times\exp\left(-\frac{|\gamma|^2}{2}+\frac{\nu\gamma^2}{2\mu}\right). \tag{A5}$$

Here, $\mu=\cosh 2r$, $\nu=\sinh 2r$, $\mu^2-\nu^2=1$, here ν is real.

APPENDIX B

The average of the Hamiltonian in Eq. (6) over the states (19) referred to one site results in $\langle\tilde{H}_L\rangle/N=H_{ph}+H_{int}$, where

$$H_{ph}=\frac{\Omega}{2CN^2}\sum_{m,n}C_{1n,m}[\cosh(4r_m(n))+1]I_n + \frac{\Omega}{CN^2}\sum_{m,n}\{1+\eta^2-2e^{-8r_m(n)}\eta \times\exp[-2|\tilde{\gamma}_{1m}(n)|^2]\}|\gamma_{1m}(n)|^2I_n + \frac{\Omega}{CN^2}\sum_{n,m}C_{1m}(n)|\gamma_{2m}(n)|^2I_n, \tag{B1}$$

$$H_{int}\equiv H_{\alpha}+H_{\beta}=\frac{1}{CN^2}\sum_{n,m}\left\{\alpha(1-\eta^2)\gamma_{1m}\sigma_{zn}-\frac{\beta}{2}[(1+\eta^2)\exp(-2|\tilde{\gamma}_{1m}|^2)+2\eta]\gamma_{2m}I_n\right\}+\text{H.c.}, \tag{B2}$$

and

$$H_T=-\frac{T}{CN^2}\sum_{n,m}C_{1m}(n)\exp[-W_m(n)]M_m(n) \equiv 2(H_{T1}I+H_{T2}i\sigma_y+H_{T3}\sigma_z+H_{T4}\sigma_x). \tag{B3}$$

Calculation of the Debye-Waller factor $\exp(-W)M$ [Eq. (23)] and of Eq. (25) is based on the formulas (A3)–(A5). We approximated the average of a product in the transfer term by a product of averages. In the continuum limit, from Eq. (A3) we receive for $W(n)$ in Eq. (B3),

$$W(n)=\frac{1}{2N}\sum_m\left(\left|\frac{d\tilde{\gamma}_{1m}(n)}{dn}\right|^2+\left|\frac{d\gamma_{2m}(n)}{dn}\right|^2\right). \tag{B4}$$

With the help of Eqs. (A4) and (A5) one obtains for $E_m(n)=\langle G_{1,m+1}G_{1m}\rangle$,

$$\begin{aligned}E_m(n)\equiv&\langle 0_{m+1},0_m|S^{-1}[r_{m+1}(n)]S^{-1}[r_m(n)]\\&\times D^{-1}[\gamma_{1,m+1}(n)]D^{-1}[\gamma_{1m}(n)](-1)^{b^{\dagger}_{1,m+1}b_{1,m+1}}\\&\times(-1)^{b^{\dagger}_{1m}b_{1m}}D[\gamma_{1,m}(n+1)]D\\&\times[\gamma_{1,m+1}(n+1)]S[r_m(n+1)]\end{aligned}$$

$$\begin{aligned}&S[r_{m+1}(n+1)]|0_m,0_{m+1}\rangle\\&=\exp(-\tfrac{1}{2}[|\tilde{\gamma}_{1m}(n)|^2+|\tilde{\gamma}_{1m}(n+1)|^2+|\tilde{\gamma}_{1,m+1}(n)|^2\\&\quad+|\tilde{\gamma}_{1,m+1}(n+1)|^2+\tilde{\gamma}_{1m}(n+1)\tilde{\gamma}_{1m}(n)\\&\quad+\tilde{\gamma}_{1,m+1}(n+1)\tilde{\gamma}_{1,m+1}(n)+\tilde{\gamma}_{1m}(n)\tilde{\gamma}_{1,m+1}(n)\\&\quad+\tilde{\gamma}_{1,m+1}(n+1)\tilde{\gamma}_{1m}(n+1)]).\end{aligned} \tag{B5}$$

In the continuum limit (B5) yields $E_m(n)\rightarrow\exp(-2|\tilde{\gamma}_m(n)|^2)$.

*Electronic address: majere@prfnw.upol.cz
†On leave of absence from the Institute of Nuclear Research UAN, Pr. Nauki 47, Kiev, Ukraine.

[1] M. D. Kaplan and B. G. Vekhter, in *Cooperative Phenomena in Jahn-Teller Crystals*, edited by V. P. Fackler (Plenum, New York, 1995).
[2] O. Gunnarson, Phys. Rev. Lett. **74**, 1875 (1995); Rev. Mod. Phys. **69**, 575 (1997).
[3] G. M. Zhao, K. Conder, H. Keller, and K. A. Müller, in *Electrons and Vibrations in Solids and Finite Systems (Jahn-Teller Effect), Berlin 1996*, edited by H. J. Schultz and U. Scherz (R. Oldenbourg Verlag, München, 1997), p. 537.
[4] A. Bill and V. Z. Kresin, in *Electrons and Vibrations in Solids and Finite Systems (Jahn-Teller Effect)* (Ref. 3), p. 545; A. Bill, V. Z. Kresin, and S. A. Wolf, Phys. Rev. B **57**, 10 814 (1998).
[5] V. Z. Kresin and S. A. Wolf, Phys. Rev. B **49**, 3652 (1994); **51**, 1229 (1995).
[6] P. S. A. Kumar, P. A. Joy, and S. K. Date, J. Phys.: Condens. Matter **10**, L269 (1998).
[7] N. Manini, E. Tosatti, and S. Doniach, Phys. Rev. B **51**, 3731 (1995).
[8] H. Zheng, D. Feinberg, and M. Avignon, Phys. Rev. B **39**, 9405 (1989).
[9] H. Zheng and A. M. Jayannavar, Solid State Commun. **74**, 1137 (1990).
[10] L. Pietronero, Europhys. Lett. **17**, 365 (1992); L. Pietronero and S. Strässler, *ibid.* **18**, 627 (1992); C. Grimaldi, L. Pietronero, and S. Strässler, Phys. Rev. Lett. **75**, 1158 (1995); Phys. Rev. B **52**, 10 530 (1995); L. Pietronero, S. Strässler, and C. Grimaldi, *ibid.* **52**, 10 516 (1995); S. Sarkar, *ibid.* **57**, 11 661 (1998).
[11] E. Capelluti, C. Grimaldi, L. Pietronero, S. Strässler, and G. A. Ummarino, cond-mat/0104457v1 (unpublished); E. Capelluti, S. Ciuchi, C. Grimaldi, L. Pietronero, and S. Strässler, cond-mat/0105351v1 (unpublished). E. Capelluti, C. Grimaldi, L. Pietronero, and S. Strässler, cond-mat/0105560v1 (unpublished).
[12] A. S. Alexandov, J. Ranninger, and S. Robaszkiewicz, Phys. Rev. B **33**, 4526 (1986).
[13] N. F. Mott, in *Polarons and Bipolarons in High-T_c-Superconductors and Related Materials*, edited by E. K. H. Salje, A. S. Alexandrov, and W. Y. Liang (Cambridge University Press, Cambridge, England, 1995), Chap. 1.
[14] T. Frank and M. Wagner, Phys. Rev. B **60**, 3252 (1999).
[15] D. Feinberg, S. Ciuchi, and F. de Pasquale, Int. J. Mod. Phys. B **4**, 1317 (1990).
[16] E. Fradkin and J. E. Hirsch, Phys. Rev. Lett. **49**, 402 (1982): E. Fradkin and J. E. Hirsch, Phys. Rev. B **27**, 1680 (1983); J. E. Hirsch and E. Fradkin, *ibid.* **27**, 4302 (1983).
[17] G.-P. Borghi, A. Girlando, A. Painelli, and J. Voit, Europhys. Lett. **34**, 127 (1995).
[18] R. H. McKenzie, J. C. Hammer, and D. W. Murray, Phys. Rev. B **53**, 9676 (1996).
[19] H. Zheng and S. Y. Zhu, Phys. Rev. B **54**, 1439 (1996).
[20] C. F. Lo, Phys. Rev. A **43**, 5127 (1991); C. F. Lo and R. Sollie, Phys. Rev. B **44**, 5013 (1991).
[21] H. Chen, Y.-M. Zhang, and X. Wu, Phys. Rev. B **40**, 11 326 (1989); **39**, 546 (1989).
[22] H. A. Jahn and E. Teller, Proc. R. Soc. London, Ser. A **161**, 220 (1937).
[23] Yu. E. Perlin and M. Wagner, in *The Dynamical Jahn-Teller Effect in Localized Systems*, edited by Yu. E. Perlin and M. Wagner (North-Holland, Amsterdam, 1984), pp. 2–20.
[24] Mary C. M. O'Brien, Am. J. Phys. **61**, 688 (1993).
[25] G. A. Gehring and K. A. Gehring, Rep. Prog. Phys. **38**, 1 (1976).
[26] M. C. M. O'Brien, in *Vibrational Spectra and Structure*, edited by J. R. During (Elsevier, Amsterdam, 1981), pp. 321–394.
[27] F. S. Ham, in *Electron Paramagnetic Resonance*, edited by S. Geschwind (Plenum, New York, 1972), pp. 1–119.
[28] M. Wagner and A. Koengeter, J. Chem. Phys. **88**, 7550 (1988).
[29] H. B. Shore and L. M. Sander, Phys. Rev. B **7**, 4537 (1973).
[30] M. Wagner and J. Vázquez-Márquez, J. Phys. C **20**, 1079 (1987).
[31] A. Köngeter and M. Wagner, J. Chem. Phys. **92**, 4003 (1990); M. Sonnek, T. Frank, and M. Wagner, Phys. Rev. B **49**, 15 637 (1994).
[32] S. M. Weber-Milbrodt, Phys. Lett. A **133**, 31 (1988); S. M. Weber and H. Büttner, Solid State Commun. **56**, 395 (1985).
[33] J. G. Bednorz and K. A. Müller, Z. Phys. B: Condens. Matter **64**, 189 (1986).
[34] R. L. Fulton and M. Gouterman, J. Chem. Phys. **35**, 1059 (1961).
[35] B. W. Shore and P. L. Knight, J. Mod. Opt. **40**, 1195 (1993); I. I. Rabi, Phys. Rev. **49**, 324 (1936); **51**, 652 (1937).
[36] E. Majerníková, Phys. Rev. B **54**, 3273 (1996).
[37] H. P. Yuen, Phys. Rev. A **13**, 2226 (1976).
[38] P. Král, J. Mod. Opt. **37**, 889 (1990).